Polymer Chemistry

Accepted Manuscript

ROYAL SOCIETY OF CHEMISTRY

www.rsc.org/polymers

Abstract

Well-defined water-soluble block copolymers poly(ethylene glycol)-*b*-poly(N-(2-hydroxypropyl)methacrylamide-*co*-N-methacryloylglycylglycine) (PEG-*b*-P(HPMA-*co*-MAGG)) with different composition and narrow polydispersity were synthesized by reversible addition-fragmentation transfer (RAFT) polymerization. The *in vivo* blood clearance and biodistribution of copolymers with different compositions were studied in normal BALB/c mice. The results showed that the electronegative copolymers were rapidly eliminated from blood and tended to accumulate in liver and spleen. However, the copolymers with neutral or small amount of negative charges showed prolonged circulation time and no specific organ uptake. Combined with the quantitative analysis of in vitro hepatocytes uptake, we conclude that this was due to the balance between (i) the electrostatic repulsion between copolymer and the cell membrane and (ii) the tendency of macrophage-like cells to capture the negative charged copolymers. This work also revealed the significant roles of PEG chain length, negative charge and molecular weight for the copolymers as anticancer drug carriers with prolonged circulation and optimal biodistribution.

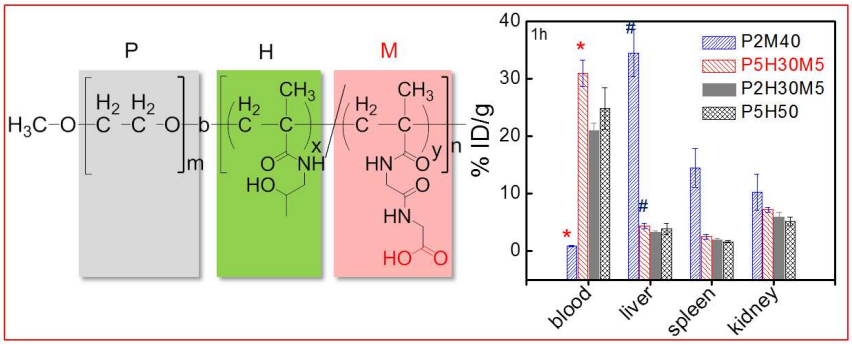

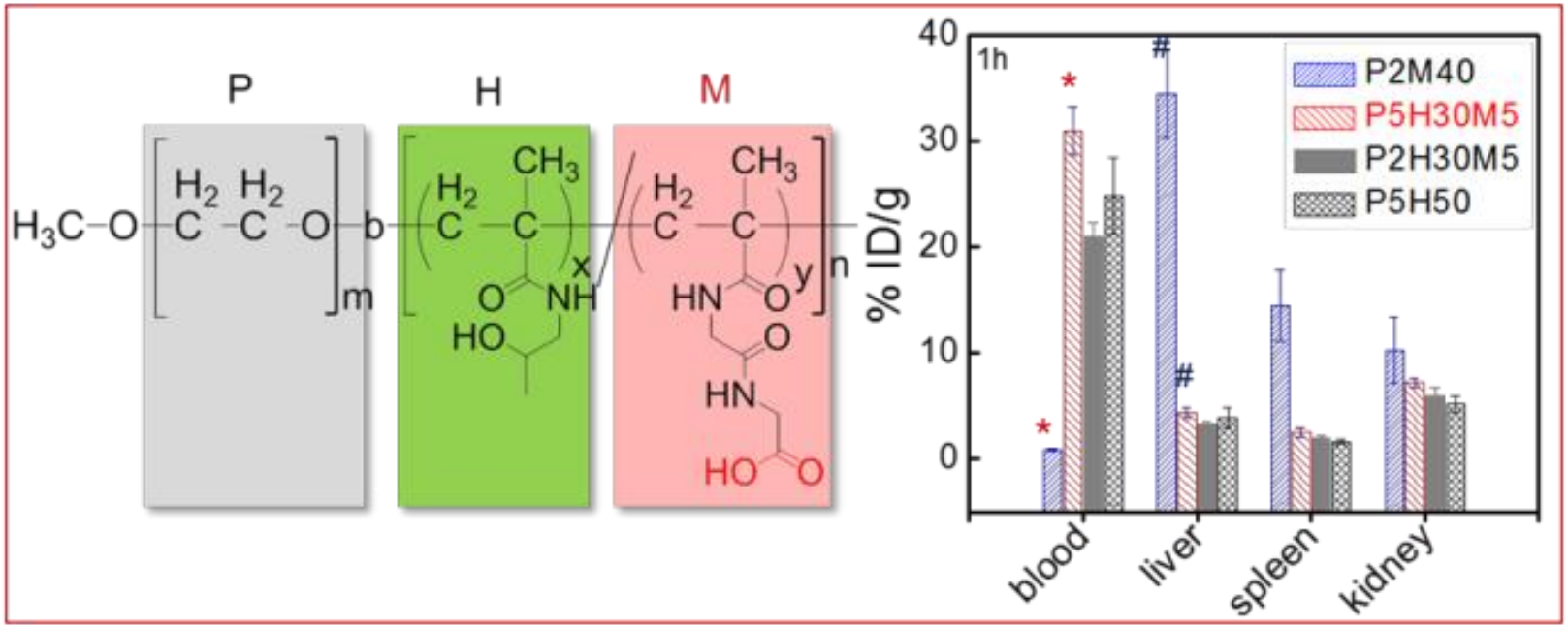

PEG-*b*-PHPMA block copolymers with precisely controlled composition were synthesized and showed good biodistribution pattern and long circulation time.

Polymer Chemistry

RSCPublishing

Full Paper

The synthesis of poly(ethylene glycol)-*b*-poly(*N*-(2-hydroxypropyl) methacrylamide) block copolymers with well-defined structure and its influence on *in vivo* circulation and biodistribution

Cite this: DOI: 10.1039/x0xx00000x

Received 00th January 2012,
Accepted 00th January 2012

DOI: 10.1039/x0xx00000x

www.rsc.org/

Qingsong Yu,‡[ab] Chengyan Dong,‡[c] Jiajing Zhang,[a] Jiyun Shi,[c] Bing Jia,[c] Fan Wang,*[c] and Zhihua Gan,*[ab]

Well-defined water-soluble block copolymers poly(ethylene glycol)-*b*-poly(*N*-(2-hydroxypropyl) methacrylamide-*co*-*N*-methacryloylglycylglycine) (PEG-*b*-P(HPMA-*co*-MAGG)) with different composition and narrow polydispersity were synthesized by reversible addition-fragmentation chain transfer (RAFT) polymerization. The *in vivo* blood clearance and biodistribution of copolymers with different compositions were studied in normal BALB/c mice. The results showed that the electronegative copolymers were rapidly eliminated from blood and tended to accumulate in liver and spleen. However, the copolymers with neutral or small amount of negative charges showed prolonged circulation time and no non-specific organ uptake. Combined with the quantitative analysis of *in vitro* hepatocytes uptake, we conclude that this was due to the balance between (i) the electrostatic repulsion between copolymer and the cell membrane and (ii) the tendency of macrophage-like cells to capture the negative charged copolymers. This work also revealed the significant roles of PEG chain length, negative charge and molecular weight for the copolymers as anticancer drug carriers with prolonged circulation time and optimal biodistribution.

1. Introduction

Historically, the administration of anticancer therapeutic agents has been limited by multiple factors, primary among these being poor solubility, low stability and rapid clearance. The consequence is short circulation half-life and low efficacy, making frequent administration necessary. Additionally, there can be significant side effects in non-diseased tissues due to the non-selective adsorption of therapeutic agent.[1,2] In order to achieve the site-specific drug delivery, macromolecular drug carriers have been investigated such as synthetic polymers,[3-5] albumin,[6] micelles,[7] nanoparticles[8,9] and liposomes.[10,11] These drug carriers can selectively accumulate in tumor regions due to the enhanced permeation and retention (EPR) effect[12] and long circulating characteristics.[13]

Polymer-drug conjugates have been widely studied for three decades as a potential solution to overcome the limitations of current chemotherapy.[3,14] The typical polymers include poly(ethylene glycol) (PEG),[15] poly(*N*-(2-hydroxypropyl) methacrylamide) (PHPMA),[16] dextran,[17,18] and polyglutamate[19] etc. PEG has been widely studied due to its non-toxic, non-immunogenic characteristics, and especially the approval by the Food and Drug Administration (FDA) for clinical application. The use of PEG for nanoparticle surface functionalization has led to very favorable results such as the resistance to non-specific adsorption of proteins and the prolonged circulation time.[20-22] Although the PEG-drug conjugates have been considered as the potential long-circulating drug delivery systems for systemic drug administration, the application is restrained by the limited number of reactive sites, low drug loading capacity[15] as well as the accelerated blood clearance (ABC) by the immune system.[23] PHPMA has also been explored as another water-soluble, inert, non-immunogenic and uncharged polymer which can be well functionalized by the copolymerization with its derivatives. It is anticipated that the integration of PEG and PHPMA may bring about a recombinant of their advantages such as better "stealth" properties, longer circulation time, lower normal organ uptake and better functionalization. Therefore, the copolymer with PEG and PHPMA components is of great potentials not only for the demonstration of the relationship between structure and biofunctions, but also for the clinical application due to the FDA approval of both components.

However, traditionally PHPMA is synthesized by free radical polymerization which leads to uncontrollable molecular weight and broad distribution, while PEG is usually synthesized by anionic ring-opening polymerization. It is unable to synthesize the block copolymer of PEG and PHPMA via traditional method. Fortunately, with the development of modern living radical polymerization techniques such as reversible addition-fragmentation chain transfer (RAFT) polymerization, the synthesis of PHPMA with well-controlled molecular weight and narrow distribution (PDI<1.1) is possible.[24,25] This technique also make the preparation of PEG-*b*-PHPMA block copolymer available.

The copolymerization of HPMA with other functional monomers can provide flexible chemical structures that allow for the conjugation of various moieties such as targeting molecules,[26,27] anti-cancer drugs,[28] fluorophores as well as ligand for radionuclide.[29] *N*-methacryloylglycylglycine (MAGG)[30] and *N*-methacryloylglycyl-phenylalanyl-leucyl-glycine (MAGFLG)[31] are commonly used comonomers for the further modification of PHPMA. MAGG can be used to conjugate anti-cancer drugs to evaluate the metabolic pathway of polymer-drug conjugates before the drug was released. However, there is still several problems exist in the study of copolymerization of HPMA and MAGG. i.e. Whether MAGG hinder the living polymerization process or can the composition be precisely controlled? Does the introduction of MAGG content have influence on the solution properties of the prepared copolymers? And whether the resultant chemical change impacts their biological functions?

It has been reported that the molecular weight (M_w), and thus hydrodynamic volume (V_h) play critical roles in pharmacokinetics (PKs) and *in vivo* biodistribution for water-soluble polymer drug conjugates.[32] Once the hydrodynamic diameter (D_h) of a polymer exceeds the renal threshold of 5nm,[33,34] the filtration rate of macromolecules decreases with increasing D_h, as long as other factors, such as molecular conformation and chemistry, remain constant. Thus the blood circulation time increases with increasing M_w as a result of decreased filtration by the kidneys.[5,35,36]

In addition to the Mw, the surface charge of drug nanocarriers has been reported to be a very important factor in determining the efficiency and mechanism of cellular uptake, as well as the *in vivo* fate. However, the optimum surface charges and charge densities were reported differently for different nanocarriers.[7,11,37] For PHPMA copolymers, the *in vivo* biodistribution and renal elimination rate are dependent on both molecular weight and charge. The neutral copolymers were found to accumulate in lung, liver and spleen, while no specific organ uptake except kidney can be found for negative copolymers.[29] The copolymers with higher molecular weight show higher uptake for all non-renal tissue (heart, lung, spleen, liver, and muscle).[38]

The aim of this work is to investigate the relationship between chemical composition and *in vivo* biofunctions for polymers as drug delivery carriers. For this purpose, the synthesis of PEG-*b*-P(HPMA-*co*-MAGG) block copolymers with well-controlled molecular weight and composition by RAFT polymerization was studied. The solution properties of the copolymers were characterized by dynamic light scattering (DLS) and capillary electrophoresis (CE). The cellular experiments and animal tests were performed to demonstrate the effects of molecular weight and negative charges of copolymers on in vitro hepatocytes uptake, PKs as well as *in vivo* biodistribution in BALB/c normal mice. The results of this work will provide an theoretical evidence for the design and synthesis of efficient polymer conjugates with long circulation time and optimal biodistribution for anticancer drug delivery.

2. Experimental section

2.1 Materials

N-(2-hydroxypropyl)methacrylamide (HPMA, reagent grade, Polysciences Inc), 4,4'-Azobis(cyanopentanoic acid) (V501, >98%, Fluka), tyrosine (Tyr, >98%, Alfa Aesar) and 4-(*N*,*N*-dimethylamino)pyridine (DMAP, 99%, Alfa Aesar), Iodogen (Sigma, St. Louis, MO), $Na^{125}I$ (Beijing Atom High Tech, Beijing, China) and PD MiniTrap column (GE Healthcare, Buckingmashine, UK) were used as received without further purification. Water (HPLC grade) was obtained with a Milli-Q system (Millipore, Bedford, MA). Sodium cholate was purchased from Sigma. Dichloromethane and acetonitrile (HPLC grade) were obtained from Acros Organics. The other chemicals (reagent grade) in this work were purchased from Aldrich and used without purification. PEG macromolecular chain transfer agent (PEG-CTA),[39] *N*-methacryloylaminopropyl fluorescein thiourea (MA-FITC)[40] and *N*-methacryloylglycylglycine (MAGG)[41] were synthesized according to the literature procedure. The NCTC-1469 murine hepatocytes were obtained from the American Type Culture Collection (ATCC; Rockville, MD).

2.2 Synthesis of methacryloyl tyrosyl methyl ester (MA-Tyr)

Tyrosyl methyl ester hydrochloride[42](2.31 g, 10.0 mmol) and triethylamine (2.22 g, 22.0 mmol) were added into dichloromethane (30mL). The solution was kept in an ice bath for 30 min. A solution of distilled methacryloyl chloride (1.04 g, 10.0 mmol) in dichloromethane(DCM) (10 mL) was added slowly to the above mixture. After the addition of methacryloyl chloride, the resultant mixture was stirred at room temperature overnight. The DCM solution was successively washed with hydrochloric acid (100 ml, 1 M), saturated sodium bicarbonate solution (100 ml) and water, dried over magnesium sulfate and then evaporated to dryness. Yield: 2.24 g (85%) pale yellow oil. ^{1}H NMR (400MHz, Acetone-d_6): δ [ppm] 7.08 (d, 2H), 6.95 (d, 2H), 5.67 (s, 1H), 5.35 (s, 1H), 4.88 (dd, 1H). 3.75 (s, 3H), 3.10 (m, 2H), 1.93 (s, 3H).

2.3 Synthesis of PEG-*b*-P(HPMA-*co*-MAGG) and PEG-*b*-P(MAGG) block copolymers

A given amount of PEG-CTA, HPMA, MAGG, MA-Tyr, MA-FITC and V501 (CTA/initiator=4/1) in DMSO was added into a

schlenk tube, degassed via three freeze−thaw cycles. The polymerization was conducted at 70 °C for 48 h. Then the polymerization was halted by immediate exposure to air and cooling with liquid nitrogen. The reaction solution was precipitated into acetone for three times to remove unreacted monomer and PEG. The final product was obtained as pink solid after drying in vacuum. Yield: 70-90 %. The chemical structure of the copolymers was analyzed by ^{1}H NMR. The number-average molecular weight (Mn) and polydispersity indices (Mw/Mn) were measured by a SHIMADZU Lc-10Avp aqueous size exclusion chromatography (SEC) equipped with SD-806HQ column in 0.1 mol/L $NaNO_3$ at a flow rate of 1.0 mL/min and at 35 °C. The fluorescence spectra of all copolymers were acquired on a Hitachi F4500 apparatus.

2.4 Capillary electrophoresis

All electrophoretic experiments were performed on a P/ACE model 2050 (Beckman, Fullerton, CA, USA) mounted with a bare fused-silica capillary of 47 cm (40 cm to detector)×50 μm id, from Yongnian Optical Fiber Factory (Hebei, China). Prior to every injection, the capillary was successively flushed with 0.1 M NaOH, water, and running buffer (10 mM phosphate buffer, pH=7.4) for 3 min each. Samples were introduced by pressure injection at 0.5 psi (1 psi = 6894.76 Pa) for 2 s and separated at +15 kV. The separated bands were detected by UV absorption at 254 nm through a slit aperture of 100×200 μm. The data were acquired at 5 Hz and processed with the P/ACE workstation. DMSO was used as the Electroosmotic flow (EOF) marker. Unless otherwise noted, the running buffer was renewed every run.

2.5 ^{125}I labeling of PEG-*b*-P(MAGG) and PEG-*b*-P(HPMA-*co*-MAGG)

The diblock copolymers were labeled at room temperature and ambient pressure with ^{125}I using the Iodogen method as previously reported.[43] Briefly, 100 μg of P2M40 and 37 MBq Na^{125}I in 0.2 M pH 7.4 phosphate buffer were added to a vial coated with 20 μg Iodogen. The molar ratio of Na^{125}I to tyrosine residues is 10~120 in the feeding reaction mixture. Generally, all the tyrosine residues can be labeled under this labeling condition. The resultant labeled copolymer was purified by a PD MiniTrap G-25 column (28-9180-07-07, GE Healthcare) equilibrated with phosphate buffer (0.2 M, pH7.4) to remove unreacted radioiodine. The radioactive fractions of ^{125}I-P2M40 were collected and passed through a 0.2 μm syringe filter for further in vivo experiments. A similar procedure was used for the rest of the copolymers. The quality control was carried out with Instant Thin-Layer Chromatography (ITLC) method using Gelman Sciences silica-gel paper strips and acetone as eluent. By this method, free ^{125}I migrated to the solvent front while ^{125}I labeled polymer remained at the origin.

2.6 Solution stability

The solution stability of all ^{125}I radiotracers was determined in saline at a final concentration of 2 mCi/mL. The samples were analyzed by ITLC at 12, 24 and 48 h.

2.7 Cell lines and cell culture

NCTC 1469 (ATCC CCL-9.1) murine normal hepatocytes were cultured in Dulbecco's Modified Eagle's Medium supplemented with penicillin, streptomycin and 10 % heat inactivated horse serum. The concentration of L-Glutamine was adjusted to 4mM. Cells were maintained at 37 °C in a humidified atmosphere of 5 % carbon dioxide and 95 % air. All tissue culture media were obtained from Gibco Life Technologies, Inc. (Grand Island, NY). Cells were used 2 days after being plated unless otherwise stated.

2.8 Animal studies

All the ^{125}I-labeled copolymers were purified using a PD MiniTrap G-25 column before animal experiments. The PD MiniTrap G-25 column was washed with 6 mL of PBS and was activated with 2 mL of 1 % BSA before purification. After that PD MiniTrap G-25 column was loaded with radiotracer (~100μL) and then washed with 4 mL of PBS, the 0.5 mL between 0.6 and 1.1 mL of eluent was collected. We prepared doses for animal studies by dissolving the purified radiotracer in 0.9 % saline to give a concentration of 100 μCi/mL for biodistribution studies and 2.5 mCi/mL for imaging. Each animal was injected with 0.1 mL of radiotracer solution (10 μCi/mouse). All animal experiments were performed in accordance with guidelines of Peking University Health Science Center Animal Care and Use Committee.

2.9 Blood clearance and biodistribution experiments

Seven BALB/c normal mice were used as one group for the blood clearance experiment of one copolymer radiotracer. The ^{125}I-labeled copolymer (10 μCi in 0.1 mL 0.9% saline) was administered intravenously to each mouse. Blood was harvested from orbital sinus at 1, 3, 5, 7, 10, 15, 20, 30, 60, 90, 120, 180, 240, 480, 1440 and 2880 min postinjection (p.i.), and the radioactivity was measured using a γ-counter (Wallac 1470-002, Perkin-Elmer, Finland). The uptakes of radiotracer in blood were calculated as the percentage of the injected dose per gram of blood mass (%ID/g).

For biodistribution studies, 16 BALB/c normal mice were randomly divided into four groups. The ^{125}I-labeled copolymer (10 μCi in 0.1 mL 0.9% saline) was administered intravenously to each mouse. Time-dependent biodistribution studies were carried out by sacrificing mice at 1, 4, 24, and 48 h postinjection. Blood, heart, liver, spleen, kidney, stomach, intestine, muscle, and bone were harvested and measured for radioactivity in a gamma counter (Wallac 1470-002, Perkin-Elmer, Finland). The organ uptake was calculated as a percentage of injected dose per gram of wet tissue mass (%ID/g).

2.10 Scintigraphic imaging

The imaging study was performed using three BALB/c normal mice. Each animal was administered with 500 μCi of ^{125}I labeled copolymers in 0.2 mL saline. Animals were anesthetized and placed supine on a three-head-camera (GE Healthcare, Millennium VG SPECT) equipped with a parallel-hole, low energy, and high-resolution collimator. Anterior images were acquired at 24 h postinjection and stored digitally in a 128×128 matrix. The acquisition count limits were set at 200 K. After completion of the imaging study, animals were sacrificed by cervical dislocation.

2.11 Isolation of murine liver cells

The karat parenchymal and non-parenchymal cells were isolated from adult mouse livers (8–14 weeks of age) after the administration of fluorescent copolymers (20 mg/kg) according to the method described in the literature.[44] Parenchymal cells were separated from non-parenchymal cells by centrifugation at a relative centrifugal force of 50 g for three times. The isolated parenchymal cells were incubated with ASGR1 Antibody (8D7) PE (Santa Cruz Biotechnology, Inc.). MCAM Antibody (P1H12) PE(Santa Cruz Biotechnology, Inc.) and anti-mouse F4/80 Antigen PE BM8 (eBioscience, Inc.) were used to stain the Liver Sinusoidal Endothelial Cells (LSEC) and Kupffer Cells (KC) in non-parenchymal portion respectively. Both the parenchymal cells and non-parenchymal cells isolated at 24 h after the injection were stained by the Goat anti Rabbit IgG1 PE (GAR IgG1 PE) and used as the isotype control. All these cells were analyzed by Accuri C6 flow cytometer (Becton & Dickinson). Cells stained with FITC or PE were used to manually compensate the PE and FITC channels. Compensation levels were set at 1.6 % PE from FITC subtraction, 20 % FITC from PE subtraction. Data analysis was performed using FCS Express 4 Flow Research edition (De Novo Software).

2.12 Cellular uptake of polymers with different amount of negative charge

For the analysis of cellular uptake by flow cytometry, NCTC-1469 cells were plated in 24-well plates (7.5 ×10^4 per well) two days prior to the experiment. Cells were treated with 200 μL of polymer solutions in FBS-free media or assay buffer. Cells were incubated for 12 h at 37 ^{o}C/5% CO_2, washed subsequently thrice with ice-cold PBS, trypsinized and centrifuged. The cell pellet was resuspended in 400 μL PBS with 1 % bovine serum albumin, split in two aliquots and analyzed using flow cytometry. Each data point was performed in triplicate. The mean fluorescence intensity was analyzed using Cell Lab Quanta SC MPL flow cytometer (Beckman Coulter). Data were acquired in linear mode and visualized in logarithmic mode. Approximately 10,000 digital list mode events were collected and the data gated on forward and side scatter parameters to exclude debris and dead cells. Cells without labeled polymers were used as the negative control for autofluorescence. Data analysis was performed using WinMDI 2.9 software.

2.13 Confocal laser scanning microscopy

Polymer uptake studies of NCTC-1469 cells were performed using a FluoView Confocal Laser Scanning Microscopes-FV1000 (Olympus, Tokyo, Japan) equipped with a 100×Olympus UPlanApo oil immersion objective (NA, 1.35). One day prior to each study, 5-10×10^4 cells were seeded on 35 mm glass-bottom dishes (Nest Biotechnology Co., Ltd., Shanghai, China). The fresh media (2 mL) containing micromolar concentrations of polymer conjugates (20 μM FITC equivalent) was added and then incubated for 12 h. Before observation, the incubation media was replaced with fresh media. The untreated cells were observed to reduce background fluorescence.

2.14 Statistical analysis

The biodistribution data and blood clearance curve are reported as an average plus the standard variation. Comparison between two different radiotracers was also made using the one-way ANOVA test (GraphPad Prism 5.0, San Diego, CA). The level of significance was set at p=0.05.

3. Results and discussion

3. 1 Synthesis of copolymers with well-defined structure

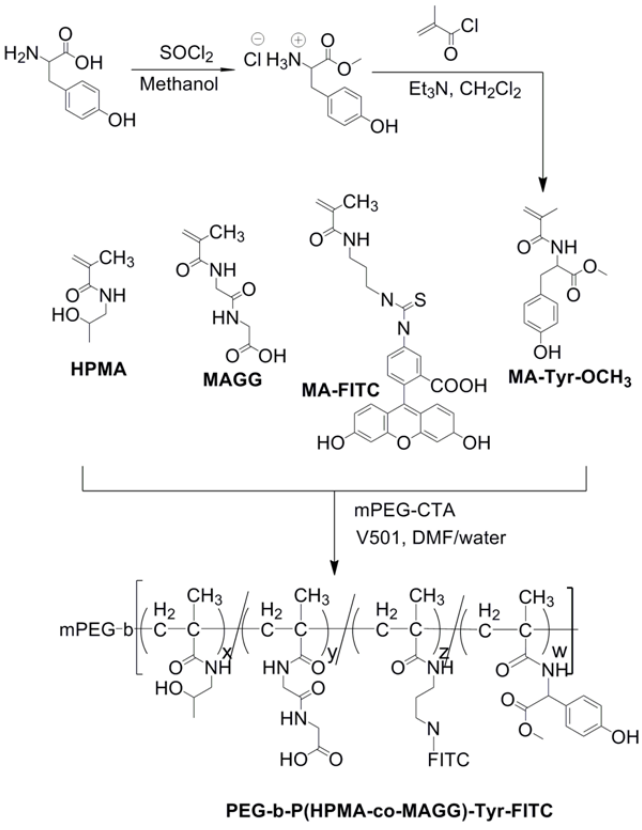

Scheme 1. Synthetic routes of MA-Tyr and PEG-*b*-P(HPMA-*co*-MAGG) copolymers.

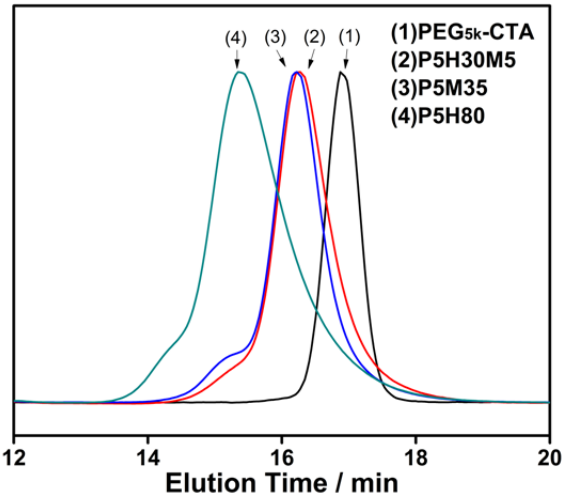

Figure 1. SEC curves of PEG_{5k}-CTA (1), P5H30M5 (2), P5M35 (3) and P5H80 (4)

Scheme 1 shows the synthetic routes of tyrosine residue contained monomer (MA-Tyr) and the copolymers composed of PEG, HPMA, MAGG, MA-Tyr and MA-FITC. The MA-Tyr and MA-FITC were synthesized for radiolabeling and fluorescent labeling, respectively. Although the copolymers with different compositions were designed, the amount of tyrosine and FITC residue was kept constant in copolymers.

Figure 1 shows the SEC results of PEG-CTA and copolymers. For the sake of clarity, the theoretical molecular weights were used in the nomenclature of the copolymers, e.g. P2M40 stands for PEG_{2k}-*b*-$PMAGG_{40k}$, P5H30M5 stands for PEG_{5k}-*b*-P($HPMA_{30k}$-*co*-$MAGG_{5k}$). Compared to the elution time of PEG_{5k}-CTA, the shorter elution time of copolymers P5M35, P5H30M5 and P5H80 indicated the successful synthesis of copolymers from macro-CTA via RAFT polymerization. The unimodal peaks and very narrow polydispersity indicated that the RAFT copolymerization of HPMA and MAGG in the presence of PEG-CTA is a well-controlled process.

Figure 2 shows the ^{1}H NMR spectra of monomer and copolymers. The appearance of peaks at 3.9 ppm, 3.6 ppm and 3.0 ppm from MAGG, PEG and HPMA respectively clearly proved the successful synthesis of copolymers. The successful introduction of tyrosine can be confirmed by the appearance of the characteristic peaks at 6.5-7.5 ppm. The contents of HPMA, MAGG and tyrosine were calculated from the integral ratio of the characteristic peaks at 3.9 ppm (MAGG), 3.6 ppm (PEG), 3.0 ppm (HPMA) and 6.8 ppm (tyrosine).

Table 1 summarizes the characterization of PEG-*b*-P(HPMA-*co*-MAGG) copolymers. The amount of FITC in the copolymers was determined by fluorescent spectrometry. The number of the repeating units of PEG_{2k} and PEG_{5k} was set as 45 and 114 respectively. From Table 1 we can find out that the theoretical and experimental values of molecular weight of each component are close to each other, indicating that the block

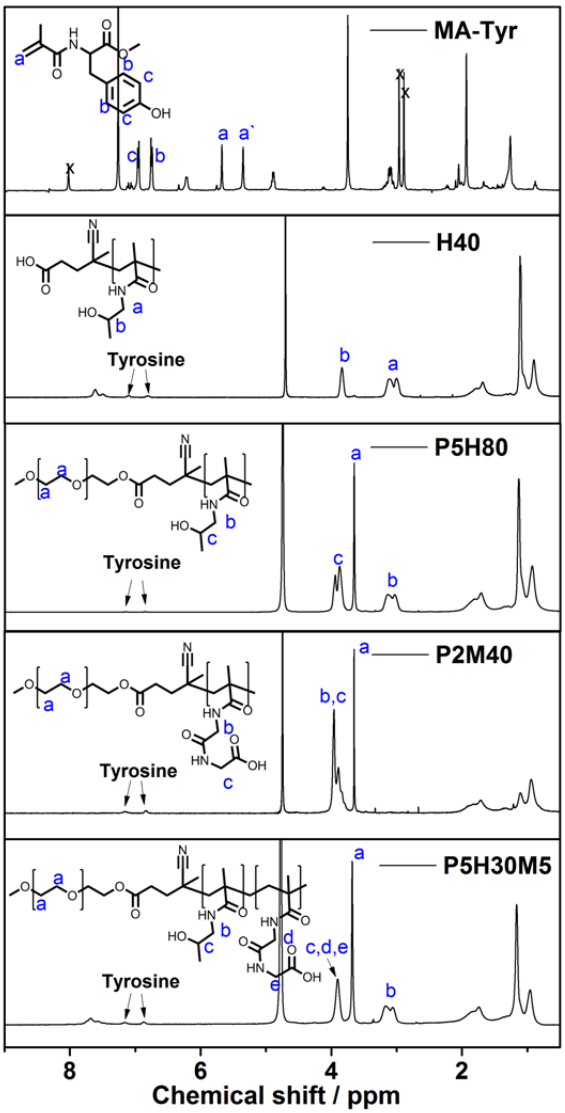

Figure 2. The representative ^{1}H NMR spectra of MA-Tyr (in acetone), H40, P5H80, P2M40 and P5H30M5 (in D_2O)

length and the content of carboxyl groups in our copolymers were precisely controlled during polymerization process by changing the molar ratio of HPMA to MAGG monomers in feed or by changing the PEG block length.

3. 2 Hydrodynamic diameter of copolymers

Based on the nature of living polymerization, a series of copolymers P2M40, P2H30M5, P5H20M15, P5H30M15, P15H25, H40, P5H50 and P5H80 with well-defined composition were synthesized to demonstrate the influence of composition on the solution behavior and biological functions. To evaluate the solution properties of these copolymers, these copolymers were tested by DLS and CE respectively.

Figure 3 shows the aggregation behavior of copolymers with different compositions in water and PBS. In aqueous solution,

Table 1. Characterization of PEG-*b*-P(HPMA-*co*-MAGG) copolymers.

Sample Name	P [a)]	H [a)]	M [a)]	Tyr [a)]	FITC [a)]	Mw [a)]	PDI [b)]	D_h(nm) [c)]
P2M40	2,000	0	45,000	6.0	2.0	47,000	1.10	8.38±0.63
P2H30M5	2,000	29,500	4,100	6.2	2.1	35,600	1.11	10.36±1.15
P5H20M15	5,000	17,900	21,600	6.1	1.9	44,500	1.13	11.69±0.77
P5H30M5	5,000	28,700	3,900	5.9	2.2	37,600	1.06	12.51±1.08
P5H50	5,000	54,000	0	5.9	2.0	59,000	1.08	8.64±0.37
P5H80	5,000	86,000	0	5.8	2.0	91,000	1.13	10.68±0.95
P15H25	15,000	23,000	0	6.3	1.9	38,000	1.07	11.54±1.31
P5M35	5,000	0	34,000	5.9	2.1	39,000	1.08	11.25±0.78
H40	0	38,000	0	6.0	2.1	38,000	1.08	10.23±0.94
P5H50 W/O Tyr [d)]	5,000	50,000	0	6.0	2.0	55,000	1.08	8.58±0.67

[a)] P represents the molecular weight of PEG; H and M represent the sum of the molecular weight of HPMA and MAGG, respectively. Tyr represents the molar ratio of tyrosine residue in P(HPMA-*co*-MAGG) block. FITC represents the molar ratio of FITC residue in P(HPMA-*co*-MAGG) block. Mw is the molecular weight of the copolymers. All of the above data were calculated from ^{1}H NMR in deuterium oxide. [b)] The polydispersity index was determined by SEC in 0.1M $NaNO_3$ (aq); [c)] The hydrodynamic diameter of the block copolymers was determined by DLS measurement in 10 mM phosphate buffer (pH=7.4). [d)] Represents P5H50 copolymer without tyrosine residue.

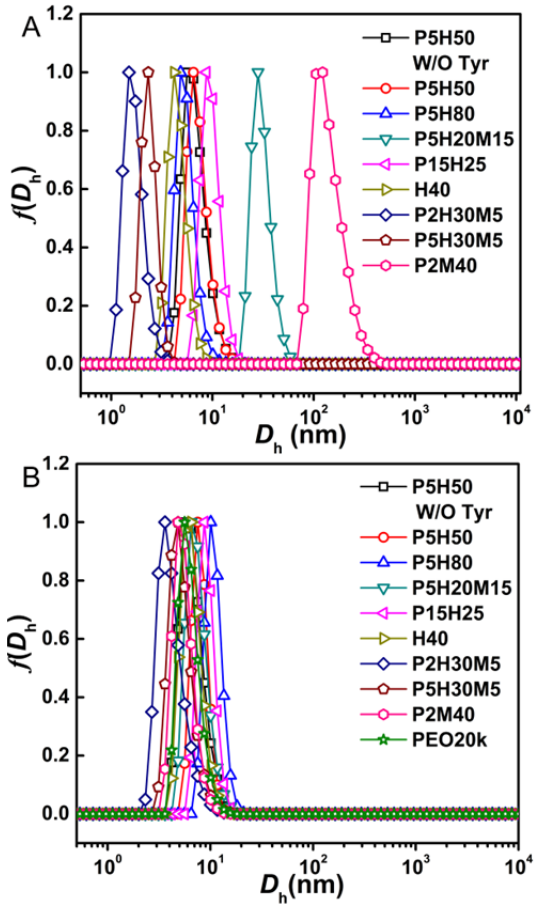

Figure 3. Hydrodynamic diameter distribution by number of block copolymers in water (A) and 10 mM phosphate buffer (pH 7.4) (B) measured by DLS at room temperature, c = 1 mg/ml.

the copolymers containing more MAGG showed larger D_h. For example, D_h of P2M40 was 150 nm, D_h of P5H20M15 was 30 nm, while D_h of P5H80 was only 10 nm. These results suggested that the copolymers with more MAGG components are aggregated in water. However, in PBS (pH 7.4, 10 mM), all copolymers showed D_h around 10 nm, suggesting that no aggregation occurred for all copolymers in PBS. In this case, the copolymers with higher molecular weight of PEG or PHPMA showed larger D_h values. Furthermore, from the D_h values of P5H50 (9.29 nm) and P5H50 W/O Tyr (9.16 nm), we can conclude that the introduction of a small amount of tyrosine and FITC shows no obvious influence on the chain conformation of copolymers in PBS.

The above phenomenon could be attributed to the different hydrophilicity of carboxyl group of MAGG in aqueous solution and PBS. It has been reported that the carboxyl groups only in buffer solution were ionized and shielded by the counterions which prevent the formation of aggregates.[6] The increased hydrophilicity and chain length of P5H80 and P15H25 copolymers also led to their larger size in PBS. Therefore, the size difference of copolymers in water and buffer solution remind us not to ignore the possible aggregation when the copolymers are injected into body, which may lead to the different PKs and biodistribution.

3. 3 Charges of copolymers with different compositions

Due to the negative charge of carboxylic group of MAGG, the change of MAGG content should bring about the alteration of the net charge of PEG-*b*-P(HPMA-*co*-MAGG) copolymers. According to the report that the micelles with different surface charges could be characterized by using agarose gel electrophoresis,[7] the net charge of copolymer was determined qualitatively by capillary electrophoresis (CE) in this work. The zeta potentials of these copolymers were also determined by zetasizer(Figure S1). These results showed similar tendency as the CE results in Figure 4.

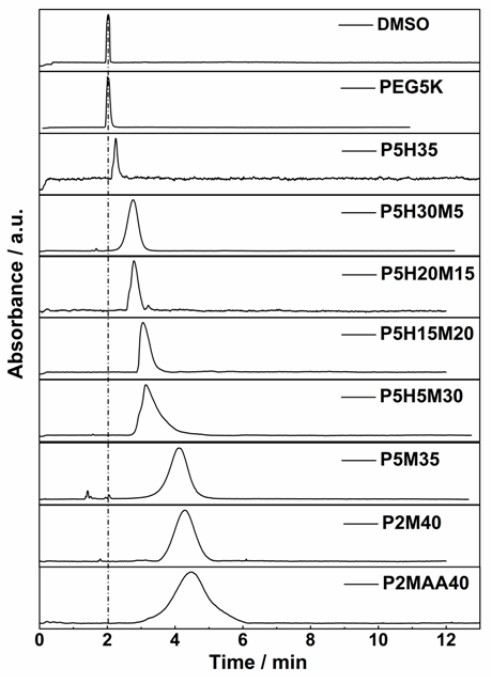

Figure 4. Capillary electrophoresis elugram of DMSO, PEG_{5k} and the block copolymers with different charge.

Figure 4 represents the electrophoretic mobility of PEG-*b*-P(HPMA-*co*-MAGG) copolymers with different amount of MAGG. The peak time of DMSO, PEG_{5k}, P5H35, P5H30M5, P5H20M15, P5H15M20, P5H5M30, P5M35, P2M40 and P2MAA40 was 2.0, 2.0, 2.2, 2.7, 2.8, 3.0, 3.2, 4.1, 4.3 and 4.5 min, respectively. DMSO was used as the electroosmotic flow (EOF) marker (neutral). The PEG_{2k}-*b*-poly(methacrylic acid)$_{40k}$ (P2MAA40) with the highest electronegativity was used as the negative control. Due to the forward voltage applied in the test, those copolymers with elution time longer than DMSO carried negative charge. The longer the elution time, the more negative the net charge.

According to the CE results in Figure 4, it can be found from these diagrams that PEG and PHPMA carried neutral charge at pH 7.4. With increasing more MAGG contents, the net charge of copolymers became more negative accordingly. Therefore the introduction of PMAGG brings negative charge to the copolymers. We can also conclude that the net charge of these copolymers can be precisely controlled by altering the molar ratio of comonomers in feed.

Based on the above results, the PEG-*b*-P(HPMA-*co*-MAGG) copolymers with well-controlled chemical composition and negative charges were successfully synthesized by RAFT copolymerization. For the further investigation on the influence of chemical composition and negative charge on the biofunctions of copolymer as anticancer drug conjugates, the PEG-*b*-P(HPMA-*co*-MAGG) block copolymers were labeled with radionuclide ^{125}I and characterized *in vivo* for blood clearance and biodistribution in normal mice. The radiolabeling efficiency for all copolymers was greater than 90 %, and the

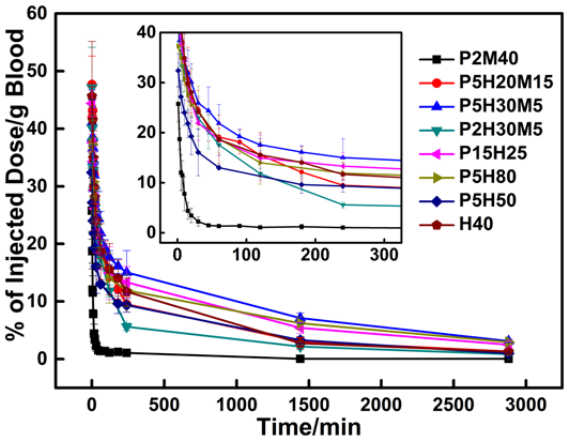

Figure 5. Blood clearance of copolymers with different charge and molecular weight in normal BALB/c mice after 48 h. Each data point represents an average of data in seven animals.

radiochemical purity (RCP) (for example ^{125}I labeled P5H30M5) after PD MiniTrap column purification was higher than 99 % (Figure S2). For all radiolabeled copolymers, it was found that their RCP values were still above 90 % after purification for 48 h, and still high enough after 72 h, around 80 %. These results revealed the stability of radionuclide labeled copolymers in saline solution, which guaranteed the further in vivo tests.

3. 4 Blood clearance

Figure 5 shows the plasma levels of copolymers over 48 h after a single injection of ^{125}I labeled copolymers in normal BALB/c mice. It was found that the plasma level of copolymers at each time point p.i. was strongly dependent on molecular weight, PEG chain length and negative charge. The plasma concentration of P2M40 with highest electronegativity as shown in Figure 4 was 25 %ID/g at 1 min p.i. and decreased bi-exponentially to essentially undetectable levels after 30 min. On the contrary, those copolymers containing less negative charge had blood clearance rate much slower than that of P2M40, e.g. the plasma level of P5H30M5 and P5H80 was still above 5 %ID/g after 48 h.

Table 2 summarizes the PK parameters of PEG-*b*-P(HPMA-*co*-MAGG) copolymers. The PK data were determined using the Kinetica v4.2 program with a two-compartment model. The adjacent R-square (R^2) was larger than 0.99. The elimination half-lives $t_{1/2}(\beta)$ of the tested copolymers were ranked as follows: P5H80 > P5H30M5 > P5H50 ≈ P15H25 > H40 > P5H20M15 > P2M40 > P2H30M5. Generally, copolymers with higher molecular weight showed longer elimination time; at the same molecular weight level, the copolymers with small amount of negative charge possessed longer elimination time than the non-charged ones. The distribution half-lives $t_{1/2}(\alpha)$ were ranked as the following order: P5H30M5 > P5H80 > P15H25 > P5H50 ≈ H40 > P5H20M15 > P2H30M5 > P2M40. It took longer time for the copolymer with small amount of

Table 2. The PK parameters of PEG-*b*-P(HPMA-*co*-MAGG) copolymers.

Sample Name	Kfast[a)] (min^{-1})	Kslow (min^{-1})	Half-life (min)		AUC [b)] (%ID·min/g)	R^2
			$t_{1/2}\alpha$	$t_{1/2}\beta$		
P2M40	0.0032	0.1501	4.1	210.5	962.6	0.990
P2H30M5	0.0087	0.1553	7.5	79.6	8069.8	0.996
P5H20M15	0.0045	0.0824	8.4	153.0	11571.7	0.991
P5H30M5	0.0007	0.0345	26.1	913.7	24563.1	0.999
P5H50	0.0011	0.0523	13.2	618.5	12298.6	0.996
P5H80	0.0006	0.0298	23.2	1054.5	20952.6	0.997
P15H25	0.0011	0.0552	18.6	606.7	19555.9	0.996
H40	0.0017	0.0521	13.2	401.2	10048.1	0.998

[a)] Kfast represents the faster rate constant and Kslow represents the slower rate constant; [b)] AUC equals the area under the %ID/g of blood curve from zero to infinite time.

negative charge to distribute into all tissues, which might be due to the electrostatic repulsion between polymer and cell membrane. The area under curve (AUC) values of the tested copolymers were ranked as follows: P5H30M5 > P5H80 > P15H25 > P5H50 > P5H20M15 > H40 > P2H30M5 > P2M40. P5H30M5 which carried small amount of negative charge and longer PEG block length possessed the largest AUC value which indicated the longest exposure time.

3. 5 *In vivo* biodistribution

Figure 6(A) illustrated the retention of copolymers in different organs/tissues such as blood, heart, lung, liver, spleen, kidney, stomach, intestine, bone and muscle at 1, 4, 24 and 48 h after intravenous administration of radio-labeled copolymers.

PEG and PHPMA themselves are loosely coiled macromolecules, and can only be slowly captured by fluid phase pinocytosis.[45] Therefore, those copolymers contain PEG and PHPMA (e.g. P5H50 and P5H80) showed low organ uptake. With the introduction of small amount of MAGG, the organ uptake was further reduced because of the electrostatic repulsion. However, when the PHPMA block of PEG-*b*-PHPMA copolymers was completely replaced by MAGG units, the results were totally different. The P2M40 was rapidly enriched in liver and spleen and consequently eliminated rapidly from plasma. Considering its negative charge with large amount, the enrichment of P2M40 might be due to the process called opsonization. The opsonin proteins tend to bind hydrophobic or charged polymers more than hydrophilic and neutral polymers to increase their recognizability to phagocytic cells,[46] resulting in the acceleration of copolymers' removal by liver and spleen. The P2M40 still showed obviously higher concentration in liver, spleen and kidney after 48 h, indicating the much slower body clearance rate of P2M40 with much negative charges compared to other copolymers.

The elimination of P5H80 with higher molecular weight was slower than its counterpart P5H50 with lower molecular weight. At the same molecular weight level, P15H25 have longer retention time than H40 due to the longer PEG length as well as larger size. These results were mainly due to the molecular weights and the hydrodynamic size which determine the possibility of copolymers to pass through the renal threshold. Therefore, from the viewpoint of efficient transportation of anticancer drug, the copolymers with slight negative charge such as P5H30M5 are the best candidates as drug conjugates with long circulation time and optimal biodistribution. Furthermore, compared with those PEG or HPMA modified Dex-g-PMAGGCONHTyr copolymers,[18] PEG-b-PHPMA copolymers in this work show longer circulation time and better biodistribution patterns.

Figure 6(B) shows a typical scintigraphic image after 4 h administration of ~500 μCi P2M40, P5H30M5, P5H80 and P2H30M5, respectively. It was clearly seen that the distribution of the radioactive signals were in agreement with the biodistribution results. The strong signals in bladder region indicated that the copolymers with molecular weight less than renal threshold (i.e. P2M40, P2H30M5 and P5H30M5) can be excreted by renal clearance. However, the copolymers with higher molecular weight (e.g. P5H80) were difficult to be removed from the body. It is noteworthy that no accumulation in heart and kidney was observed for these copolymers, indicating that, if used as drug conjugates, these copolymers have long circulation time in blood and finally can be effectively cleared by renal system without heart- or kidney-toxicity.[47]

3. 6 *In vitro* hepatocytes uptake

The flow cytometric assays of the uptake of P2M40 in isolated liver tissue (Figure S3) have showed that the hepatocytes play very important role in the uptake of negatively charged copolymers. As a kind of macrophage-like cells,[48,49] hepatocytes favor the more charged polymer as shown in previous work.[7,50,51] In order to demonstrate the influences of negative charge of copolymers on biodistribution, the hepatocytes endocytosis of copolymers with precisely controlled negative charges were studied by incubation with NCTC-1469 cells.

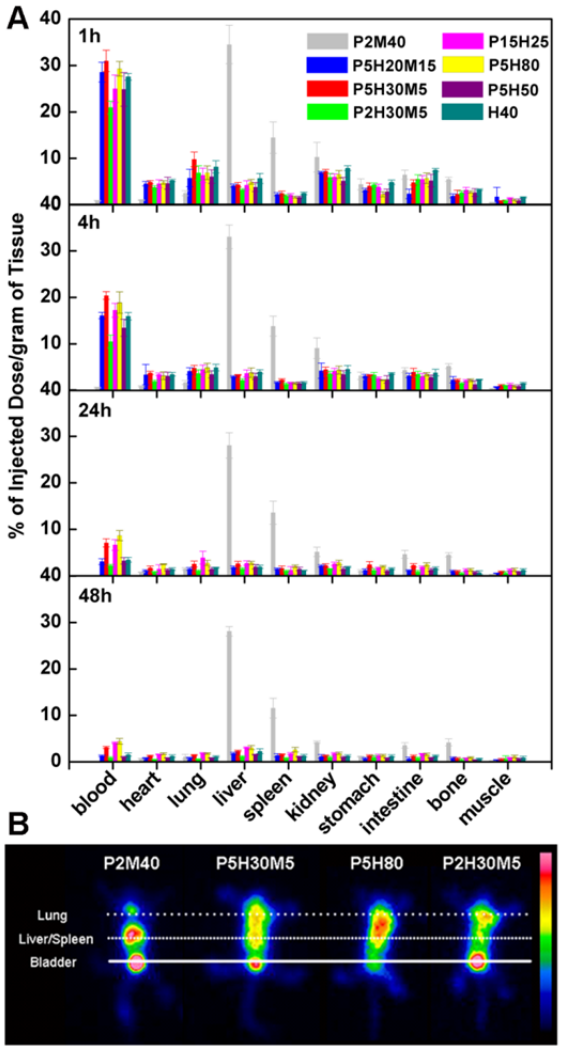

Figure 6. (A) Histograms of biodistribution data for ^{125}I labeled copolymers with different charge and molecular weight in normal BALB/c mice at 1, 4, 24 and 48 h. The organ uptake was calculated as a percentage of Injected Dose per gram of tissue (%ID/g). Each data point represents an average of data in four animals. (B) Scintigraphic images of normal BALB/c mice administered with P2M40, P5H30M5, P5H80 and P2H30M5 copolymers.

Figure 7 represents the mean values of cell associated fluorescence from three parallel experiments calibrated by the fluorescence spectra. The flow cytometric histograms and the fluorescent spectra can be found in the supplementary data (Figure S5). It was found that the net charge of copolymers significantly affected their uptake by murine hepatocytes. The negative control P2MAA40 which carried the highest amount of negative charge showed the highest uptake level. With decreasing the negative charge, the cell uptake decreased accordingly. Exceptionally, the neutral copolymer P5H35 showed uptaking level higher than P5H30M5, P5H20M15 and P5H15M20, indicating that small amount of negative charge

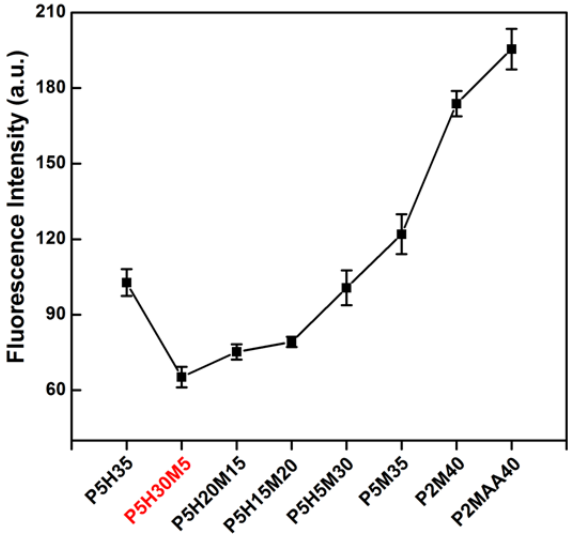

Figure 7. The influence of negative charge on the *in vitro* hepatocytes uptake. Copolymer concentration was set as 50 μg/ml

reduced the hepatocytes uptake. These quantitative results indicated again that small amount of negative charge is beneficial for preventing hepatocytes uptake due to the electrostatic repulsion, and therefore endow copolymer conjugates with long circulation time in blood for delivering drug efficiently to the cancer site.

This can also be confirmed by the confocal microscopic images, as shown in Figure 8. The copolymers with slightly negative charges (e.g., P5H30M5 and P5H20M15) showed the least and punctate distribution of the green fluorescence, while the copolymers with more negative charges such as P2M40 and P2MAA40 showed strong fluorescence distribution.

The above results revealed that the extension of circulation time for the copolymers with slightly negative charge may involve a balance between (i) the electrostatic repulsion between copolymer and the cell membrane and (ii) the tendency of macrophage-like cells to capture the negative charged copolymers.

4. Conclusion

The PEG-*b*-P(HPMA-*co*-MAGG) with well-defined molecular weight and composition were successfully synthesized by RAFT copolymerization. Based on the precisely controlled chemical structure, the influences of chemical composition and negative charge on blood clearance and *in vivo* biodistribution were studied. It was found that the increased molecular weight of copolymer and PEG chain length will lead to the prolonged circulation time and lower organ uptake. Meanwhile, slightly negative charge helps to avoid the nonspecific organ uptake. The quantitative analysis from *in vitro* hepatocytes uptake test revealed that the copolymers with small amount of negative charge are easier to escape from

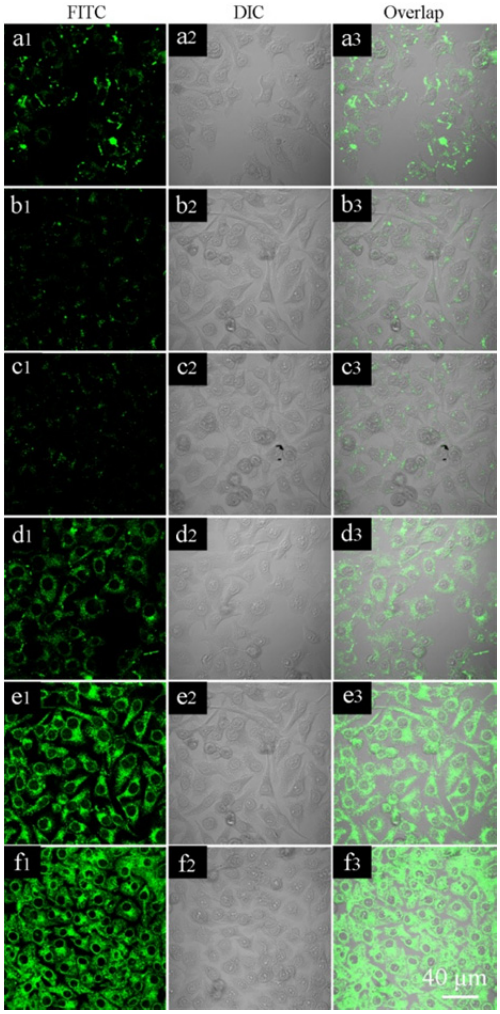

Figure 8. The confocal microscopic images of NCTC-1469 cells treated by copolymers with different negative charge: (a) P5H35, (b) P5H30M5, (c) P5H20M15, (d) P5H5M30, (e) P2M40 and (f) P2MAA40. Cells were incubated with 50 μg/ml copolymers for 4 h.

hepatocytes uptake due to the electrostatic repulsion, while too much negative charge makes the copolymer more accessible to the hepatocytes. In summary, for PEG-*b*-P(HPMA-*co*-MAGG) copolymers as potential efficient anticancer drug carriers, the introduction of small amount of negative charge is of great important for the copolymer conjugates with prolonged circulation and optimal biodistribution.

Acknowledgements

This work was supported by the Outstanding Youth Fund (Grant no. 51025314), the National Natural Science Foundations of China (Grant no. 51390481, 50873109, 50830103, 30930030), the Knowledge Innovation Program of the Chinese Academy of Sciences (Grant No KJCX2-YW-H19), and 973 project (2011CB707703) from the Ministry of Science and Technology of China.

Notes and references

[a] *The CAS Key Laboratory of Engineering Plastics, Institute of Chemistry, Chinese Academy of Sciences (CAS), Beijing100190, China. Tel +86-10-64432762, Fax: +86-10-64432762, Email: zhgan@mail.buct.edu.cn (Zhihua Gan).*
[b] *State Key Laboratory of Organic-inorganic Composites, Beijing Laboratory of Biomaterials, College of Life Science and Technology, Beijing University of Chemical Technology, Beijing 100029, China.*
[c] *Medical Isotopes Research Center, Peking University, Beijing 100191, China. wangfan@bjmu.edu.cn (F. Wang).*
[d] *University of Chinese Academy of Sciences, Beijing 100043, China.*
† Electronic Supplementary Information (ESI) available: The raw data of zeta potentials, ITLC chromatograms, The flow cytometric data of liver cell uptake, The flow cytometric histograms of hepatocytes uptake, The fluorescence spectra. See DOI: 10.1039/b000000x/
‡ These authors contribute equally to this work.

(1). Alexis, F.; Pridgen, E.; Molnar, L. K.; Farokhzad, O. C., *Mol Pharmaceut* **2008,** 5, (4), 505-515.
(2). Wu, A. M.; Senter, P. D., *Nat Biotechnol* **2005,** 23, (9), 1137-1146.
(3). Duncan, R.; Kopecek, J., *Adv Polym Sci* **1984,** 57, 51-101.
(4). Seymour, L. W.; Duncan, R.; Strohalm, J.; Kopecek, J., *J Biomed Mater Res* **1987,** 21, (11), 1341-1358.
(5). Yamaoka, T.; Tabata, Y.; Ikada, Y., *J Pharm Sci* **1994,** 83, (4), 601-6.
(6). Kratz, F., *Top Curr Chem* **2008,** 283, 73-97.
(7). Xiao, K.; Li, Y.; Luo, J.; Lee, J. S.; Xiao, W.; Gonik, A. M.; Agarwal, R. G.; Lam, K. S., *Biomaterials* **2011,** 32, (13), 3435-46.
(8). Gref, R.; Minamitake, Y.; Peracchia, M. T.; Trubetskoy, V.; Torchilin, V.; Langer, R., *Science* **1994,** 263, (5153), 1600-1603.
(9). Stolnik, S.; Illum, L.; Davis, S. S., *Adv Drug Deliver Rev* **1995,** 16, (2-3), 195-214.
(10). Campbell, R. B.; Fukumura, D.; Brown, E. B.; Mazzola, L. M.; Izumi, Y.; Jain, R. K.; Torchilin, V. P.; Munn, L. L., *Cancer Res* **2002,** 62, (23), 6831-6.
(11). Levchenko, T. S.; Rammohan, R.; Lukyanov, A. N.; Whiteman, K. R.; Torchilin, V. P., *Int J Pharm* **2002,** 240, (1-2), 95-102.
(12). Maeda, H.; Nakamura, H.; Fang, J., *Adv Drug Deliver Rev* **2013,** 65, (1), 71-79.
(13). Yamamoto, Y.; Nagasaki, Y.; Kato, Y.; Sugiyama, Y.; Kataoka, K., *J Control Release* **2001,** 77, (1-2), 27-38.
(14). Jaroslav Kálal, J. D., Jindřich Kopeček, Josef Exner, *British Polymer Journal* **1978,** 10, (2), 111-114.
(15). Veronese, F. M.; Schiavon, O.; Pasut, G.; Mendichi, R.; Andersson, L.; Tsirk, A.; Ford, J.; Wu, G.; Kneller, S.; Davies, J.; Duncan, R., *Bioconjugate Chem* **2005,** 16, (4), 775-784.
(16). Duncan, R.; Hume, I. C.; Kopeckova, P.; Ulbrich, K.; Strohalm, J.; Kopecek, J., *J Control Release* **1989,** 10, (1), 51-63.
(17). Wang, D. Q.; Shi, J. Y.; Tan, J. J.; Jin, X.; Li, Q. M.; Kang, H. L.; Liu, R. G.; Jia, B.; Huang, Y., *Biomacromolecules* **2011,** 12, (5), 1851-1859.
(18). Wang, D. Q.; Liu, R. G.; Che, N.; Li, Q. M.; Li, Z.; Tian, Y.; Kang, H. L.; Jia, B.; Huang, Y., *Polymer Chemistry* **2011,** 2, (8), 1872-1878.
(19). Schilsky, R. L.; Bailey, B. D.; Chabner, B. A., *P Natl Acad Sci-Biol* **1980,** 77, (5), 2919-2922.

(20). Stolnik, S.; Illum, L.; Davis, S. S., *Adv Drug Deliver Rev* **2012,** 64, 290-301.
(21). Bei, J. Z.; Wang, Z. F.; Wang, S. G., *Chinese J Polym Sci* **1995,** 13, (2), 154-161.
(22). Chen, L.; Zhuang, X. L.; Sun, G. E.; Chen, X. S.; Jing, X. B., *Chinese J Polym Sci* **2008,** 26, (4), 455-463.
(23). Dams, E. T. M.; Laverman, P.; Oyen, W. J. G.; Storm, G.; Scherphof, G. L.; Van der Meer, J. W. M.; Corstens, F. H. M.; Boerman, O. C., *J Pharmacol Exp Ther* **2000,** 292, (3), 1071-1079.
(24). Li, Y. T.; Armes, S. P., *Angew Chem Int Edit* **2010,** 49, (24), 4042-4046.
(25). Hong, C. Y.; You, Y. Z.; Pan, C. Y., *J Polym Sci Pol Chem* **2006,** 44, (8), 2419-2427.
(26). Borgman, M. P.; Coleman, T.; Kolhatkar, R. B.; Geyser-Stoops, S.; Line, B. R.; Ghandehari, H., *J Control Release* **2008,** 132, (3), 193-199.
(27).Mitra, A.; Mulholland, J.; Nan, A.; McNeill, E.; Ghandehari, H.; Line, B. R., *J Control Release* **2005,** 102, (1), 191-201.
(28). Caiolfa, V. R.; Zamai, M.; Fiorino, A.; Frigerio, E.; Pellizzoni, C.; d'Argy, R.; Ghiglieri, A.; Castelli, M. G.; Farao, M.; Pesenti, E.; Gigli, M.; Angelucci, F.; Suarato, A., *J Control Release* **2000,** 65, (1–2), 105-119.
(29).Mitra, A.; Nan, A.; Ghandehari, H.; McNeill, E.; Mulholland, J.; Line, B. R., *Pharmaceut Res* **2004,** 21, (7), 1153-1159.
(30). Line, B. R.; Mitra, A.; Nan, A.; Ghandehari, H., *J Nucl Med* **2005,** 46, (9), 1552-1560.
(31). Pimm, M.; Perkins, A.; Duncan, R.; Ulbrich, K., *J Drug Target* **1993,** 1, (2), 125-131.
(32). Fox, M. E.; Szoka, F. C.; Frechet, J. M. J., *Accounts Chem Res* **2009,** 42, (8), 1141-1151.
(33). Venkatachalam, M. A.; Rennke, H. G., *Circulation Research* **1978,** 43, (3), 337-47.
(34). Duncan, R., *Nat Rev Drug Discov* **2003,** 2, (5), 347-60.
(35). Kaneo, Y.; Uemura, T.; Tanaka, T.; Kanoh, S., *Biological & pharmaceutical bulletin* **1997,** 20, (2), 181-7.
(36).Kaminskas, L. M.; Boyd, B. J.; Karellas, P.; Krippner, G. Y.; Lessene, R.; Kelly, B.; Porter, C. J., *Mol Pharm* **2008,** 5, (3), 449-63.
(37). Juliano, R. L.; Stamp, D., *Biochem Biophys Res Commun* **1975,** 63, (3), 651-8.
(38). Kissel, M.; Peschke, P.; Subr, V.; Ulbrich, K.; Schuhmacher, J.; Debus, J.; Friedrich, E., *PDA J. Pharm. Sci. Technol.* **2001,** 55, (3), 191-201.
(39). Shi, L. J.; Chapman, T. M.; Beckman, E. J., *Macromolecules* **2003,** 36, (7), 2563-2567.
(40). Omelyanenko, V.; Kopeckova, P.; Gentry, C.; Kopecek, J., *J Control Release* **1998,** 53, (1-3), 25-37.
(41). Rejmanova, P.; Labsky, J.; Kopecek, J., *Makromol Chem* **1977,** 178, (8), 2159-2168.
(42). Bastiaans, H. M. M.; vanderBaan, J. L.; Ottenheijm, H. C. J., *J Org Chem* **1997,** 62, (12), 3880-3889.
(43). Fraker, P. J.; Speck, J. C., Jr., *Biochem Biophys Res Commun* **1978,** 80, (4), 849-57.
(44). Goncalves, L. A.; Vigario, A. M.; Penha-Goncalves, C., *Malaria J* **2007,** 6.
(45). Putnam, D.; Kopecek, J., *Biopolymers Ii* **1995,** 122, 55-123.
(46). Owens, D. E.; Peppas, N. A., *Int J Pharm* **2006,** 307, (1), 93-102.
(47). Yeung, T.; Hopewell, J.; Simmonds, R.; Seymour, L.; Duncan, R.; Bellini, O.; Grandi, M.; Spreafico, F.; Strohalm, J.; Ulbrich, K., *Cancer Chemother. Pharmacol.* **1991,** 29, (2), 105-111.
(48). Van Loveren HU, V. D. Z. B., De Weger RA, Van Basten C, Pijpers H, Hilgers J, Den Otter W., *J Reticuloendothel Soc.* **1981,** 29, (6), 433-440.
(49). De Weger RA, V. L. H., Van Basten CD, Oskam R, Van Der Zeijst BA, Den Otter W., *J Reticuloendothel Soc.* **1983,** 33, (1), 55-66.
(50). Jansen, R. W.; Molema, G.; Ching, T. L.; Oosting, R.; Harms, G.; Moolenaar, F.; Hardonk, M. J.; Meijer, D. K. F., *Journal of Biological Chemistry* **1991,** 266, (5), 3343-3348.
(51). He, C. B.; Hu, Y. P.; Yin, L. C.; Tang, C.; Yin, C. H., *Biomaterials* **2010,** 31, (13), 3657-3666.